DOI: 10.21062/mft.2022.065 http://www.journalmt.com

Study on Ti_2AlC/Mg Matrix Composites with Dual-scale Three-dimensional Network

Yujia Chen (0000-0002-9660-9536)[1] and Lai Hu (0000-0002-1891-2716)[2,*]
[1] The 9th Research Institute of CETC, Mianyang 621000, China.
[2] School of Mechanical Engineering, Xi'an Jiaotong University, 28 Xianning Road, Xi'an, Shaanxi 710049, P.R. China. *Condensing e-mail: Lai Hu: Laifinial@163.com.

The properties and microstructure of composites are closely related to the evolution of interface bonding. In this study, the microstructure of Ti_2AlC/Mg matrix composites with double-scale three-dimensional network was studied. The composites presented a three-dimensional network at macro and micro scales, and the matrix and reinforcements were connected with each other. The mechanical properties and damping properties of Ti_2AlC/Mg matrix composites and magnesium alloy matrix with double-scale three-dimensional network were tested. In addition, according to the basic properties of Ti2AlC/Mg ceramics and AZ91D magnesium alloy, the equivalent modulus of three-dimensional network Ti_2AlC/Mg matrix composites at micro scale was predicted by finite element method. The conclusions were as follows: (1) The ultimate flexural strength of the composites was about 10% higher than that of the matrix magnesium alloy, and the ability to maintain strength was greatly improved compared with that of the matrix magnesium alloy. (2) Using the extracted information, the equivalent modulus of the composite microscopic model was calculated to be 31.26 GPa, which is consistent with the experimental results. It provides data and theoretical support for similar research.

Keywords: Double-scale three-dimensional network; Ti_2AlC/Mg matrix composites; Magnesium alloy; Comprehensive performance

1 Introduction

Magnesium and magnesium alloys as one of the best damping metal structural materials have a series of advantages such as low density high specific strength strong damping vibration and noise reduction good electromagnetic shielding rich resources and easy to recycle. It is expected to meet the great demand of light weight, high performance and high damping metal structural materials in military and civilian fields such as weapons and equipment, aerospace and transportation equipment [1-2]. However, the damping of magnesium alloys at room temperature is mainly caused by dislocation mechanism [3-4]. So the contradiction between damping properties and mechanical properties has not been well solved.

At present, TiC, SiC, Al_2O_3 and other ceramic reinforcing phases are generally used in magnesium-based damping composites. Ceramic body mainly provides reinforcement, while magnesium matrix mainly provides damping performance. SRIKANTH et al. [5] added nano-Al_2O_3 particles to pure magnesium. When the content of nano-Al_2O_3 particles was 0.4%, the damping performance of magnesium matrix composites at room temperature was 34% higher than that of pure magnesium. The in-situ synthesis of TiC reinforced magnesium matrix composites has been studied by the researchers in [6] and [7]. They found that the introduction of TiC can improve the damping performance of matrix materials, and two damping peaks appeared in the damping-temperature spectrum of composites. WU et al. [8-9] found a similar damping phenomenon in magnesium matrix composites added with graphite particles. The damping performance of magnesium matrix composites was not advantageous at room temperature, but obviously superior to that of matrix materials at high temperature. GU et al. [10] studied the damping behavior of SiC particle reinforced magnesium matrix composites coated with Cu. The results show that the low temperature damping performance of magnesium matrix composites was lower than that of pure magnesium, but the high temperature damping performance was obviously improved. The activation energies of the two damping peaks in the damping-temperature spectrum are calculated to be 1.07 eV and 0.9 eV, respectively.

Different from the common ceramic reinforcing phase, the ternary MAX phase developed in the past ten years has the characteristics of both metal and ceramic, and has good damping performance. It is expected to become an ideal reinforcing phase for high-performance damping metal structural materials. BARSOUM [11-12] systematically studied the bending non-linear elastic deformation mechanism of

Ti_2AlC/Mg, and believed that kinkbands and delamination were the main mechanisms for this kind of ternary MAX phase to have certain ductility. ZHANG [13] prepared (AlN + Mg_2Si)/Mg Mg matrix composites reinforced by AlN particles and Mg_2Si particles by in-situ synthesis. The effect of reinforced particle size on damping properties of magnesium matrix composites at room temperature was studied. Trojanová et al. [14] used squeeze casting method to reinforce AX41 magnesium alloy with Saffil short fiber (alumina short fiber). Finally, Al_2O_3/AX41 magnesium matrix composite with Saffil short fiber content of 20% was prepared. The experimental results show that the damping performance of the composite reaches the best at 310℃. However, when the temperature was higher than 310℃, its damping performance decreased with the increase of temperature.

AZ91D is a kind of Magnesium alloy with excellent damping performance, but its low strength and easily deformation at high temperature have always been obstacles to its applications. Ti_2AlC/Mg, which was reported as a promising reinforcement material, has perfect mechanical properties and good damping performance. It can be totally believed that if the Ti_2AlC/Mg reinforcement phase was introduced into the AZ91D magnesium alloy matrix and formed with macroscopic-microscopic double-scale three-dimensional network structure, a composite material with excellent damping-strength comprehensive properties can be obtained. At present, there are not many researches on Ti_2AlC/Mg -based composite materials with three-dimensional network structure. SHAHRAM et al. [12] fabricated 50% Ti_2AlC/Mg reinforced three-dimensional network Ti_2AlC/Mg composites. It was verified that the composite had good combination of mechanical properties and damping properties. The composite material had incomparable damping performance at 500 MPa level than other crystal materials. Although three-dimensional network magnesium matrix composites have great application prospects and research value as new lightweight and high performance structural damping materials, their synthesis process, microstructure control, damping generation and coupling mechanism still need to be further studied. In this study, Ti_2AlC/Mg (MAX phase) was introduced into AZ91D magnesium alloy to prepare Ti_2AlC/AZ91D composite with macroscopic-microscopic double-scale three-dimensional network structure. The relationship between mechanical properties, damping properties and microstructure of the composite was studied, and the strengthening and damping mechanism of the composite was analyzed.

2 Methods and materials

The molten metal infiltration method is widely used in the preparation of metal matrix composites [15-16]. The magnesium liquid infiltration method is not only reliable and stable, but also easy to tun the properties. Therefore, the Ti_2AlC/Mg matrix composites with double-scale three-dimensional network were prepared by infiltration method.

2.1 Theoretical behavior analysis of Ti2AlC/Mg interface wetting

The key of molten metal infiltration is the wettability between liquid metal and ceramics. During the whole infiltration experiment, the metal experienced solid-liquid-solid changes. Porous ceramics also experienced expansion-contraction changes. In the microstructure of Ti_2AlC/Mg double-scale porous ceramic skeleton, there are not only micro-pores with different shapes, but also criss-crossing voids. These gaps are similar to capillaries, which are important ways for magnesium liquid to enter the microscopic pores of ceramic skeleton, as shown in Fig. 1.

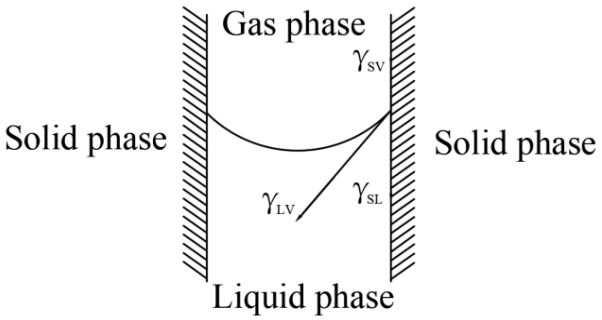

Fig. 1 *Surface tension diagram between gas phase/liquid phase/solid phase at microscopic gap*

During the infiltration process, when the magnesium liquid passes through the microscopic gap, the magnesium liquid will flow in the gap wall under the action of capillary force. If the magnesium liquid shows good wettability between the ceramic and the magnesium liquid, the capillary force is the motive force for the magnesium liquid to penetrate into the microscopic pores, and increases with the enhancement of wettability. If there is poor wettability between the two, the capillary force is the resistance of magnesium liquid to penetrate into microscopic pores.

The gap was equivalent to a capillary tube, as shown Eq. (1) [17]:

$$F = \frac{4\gamma_{LV}\cos\theta}{d} \tag{1}$$

Where:

d …The diameter of the capillary tube.

From Eq. (1), it is easy to know that capillary force is affected by wetting angle, surface tension between liquid phase and solid phase, and capillary diameter.

When the experimental temperature reaches the

melting point of the metal, the metal is molten and the porous ceramic is solid. Therefore, it can be equivalent to a dynamic model of the movement of liquid in a solid porous medium, as shown in Eq. (2) [18].

$$L = \frac{1}{\pi}\sqrt{\frac{\gamma d \cos\theta}{\eta}t} \quad (2)$$

Where:

L …The infiltration depth,

γ …The surface tension of liquid droplets on the solid,

d …That diameter of the capillary tube in the solid,

η …The kinematic viscosity between liquid and solid,

t …That residence time of the liquid in the solid hole.

2.2 No pressure and negative pressure assistance under atmosphere conditions.

The preparation of ceramic phase reinforced magnesium matrix composites by pressureless infiltration has the advantages of simple process and strong operability. In this study, six groups of experimental groups with the highest infiltration temperature and the holding time at the highest temperature increasing item by item were set up. The specific parameters and results were shown in Tab. 1.

Tab. 1 *Parameters of infiltration process in atmosphere.*

No.	Highest temperature /℃	Vacuum degree /Pa	Heat preservation time /min	Results
1	590	1.01×10^5	10	Incomplete melting
2	620	1.01×10^5	20	melted but poor infiltration
3	650	1.01×10^5	30	Melted but poor infiltration
4	680	1.01×10^5	40	Melted but not completely infiltrated
5	710	1.01×10^5	50	Melted but not completely infiltrated
6	740	1.01×10^5	60	Melted but not completely infiltrated

For the Tab. 1, when the temperature in the furnace reaches about 590℃, the magnesium alloy starts to melt, but the magnesium alloy was hardly infiltrated into the ceramic plate. Therefore, the highest infiltration temperature should be higher than 590℃. However, when the highest temperature in the furnace reaches 680℃ and the holding time was more than 40min, the infiltration effect of magnesium alloy on porous ceramic plates did not increase much with the increase of the highest furnace temperature and holding time. Therefore, the influence of auxiliary negative pressure on infiltration was further studied.

For the infiltration experiment under atmosphere conditions, it can be seen that the wetting of Ti_2AlC/Mg ceramics by Mg under argon conditions was not ideal. For Eq. (3) of infiltration capillary force principle, it can be seen that under negative pressure, the pressure inside the ceramic microscopic pores will be greatly reduced, which was very beneficial to the infiltration of magnesium liquid. Considering that magnesium liquid was easy to vaporize under too high negative pressure, only a short negative pressure was applied after the heat preservation and before solidification occurs. The highest infiltration temperature was 720℃, the infiltration time was 50min, and the final vacuum degree was 0.41 × 103 Pa. Then, five groups of infiltration pressures were set, and the experimental groups with different temperature values were extracted in the negative pressure furnace.The specific parameters and results were shown in Tab. 2.

Tab. 2 *Parameters of negative pressure assisted infiltration process.*

No.	Pressure /MPa	Extraction negative pressure temperature /℃	Vacuum degree /Pa	Results
1	0.2	590	0.41×10^3	Partial contact
2	0.4	620	0.41×10^3	Holes
3	0.6	650	0.41×10^3	Partial disappeared but successful infiltration
4	0.8	680	0.41×10^3	Partial disappearance and extrusion
5	1.0	710	0.41×10^3	Completely disappeared

For the Tab. 2, it can be seen that the magnesium liquid infiltration process was finally determined as follows: under argon atmosphere and infiltration pressure of 0.6 MPa, the temperature was increased from 10℃/min to 300℃, and the temperature was increased from 20℃/min to 720℃. After holding at 720℃ for 50min, the negative pressure was extracted at 640℃ and kept at 0.41 × 103 Pa until the end of furnace cooling.

3 Results and discussion

3.1 Characterization

(1) Macro-structural characteristics

The Fig. 2 shown a macro structure diagram of the composite material. It can be seen that no cracks can be seen by naked eyes in the magnesium alloy matrix part of the composite material and the composite material part with a three-dimensional network on the microscopic scale. From the center of the round matrix magnesium alloy to the four sides of the composite material, there was obvious color gradual change. The matrix magnesium had good bonding with the macro-circumferential interface of the surrounding materials and no pores were generated. However, these were not enough to explain that the magnesium liquid was fully infiltrated into the tiny holes and gaps in the porous three-dimensional network ceramic plate during the preparation of the composite material. Therefore, it was necessary to further analyze the microstructure characteristics of the composite materials.

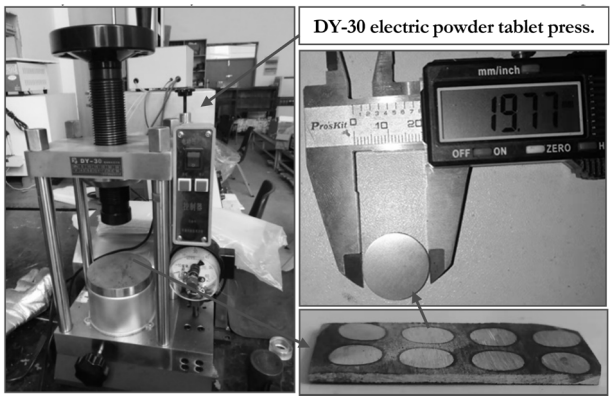

Fig. 2 *Macrostructure of Ti_2AlC/Mg matrix composites with double-scale three-dimensional network*

(2) Microstructure characteristics

The microstructure of the composite material under an optical microscope was shown in Fig. 3. It can be seen that the structure of the composite material is uniform. The microscopic pores of Ti_2AlC/Mg ceramics were filled with AZ91D. The interface between Ti_2AlC/Mg ceramics and AZ91D magnesium alloy matrix was well bonded, and the interface bonding was tight, smooth and clean, and there were no defects such as cracks. This shown that magnesium alloy had good wettability with Ti_2AlC/Mg ceramics under high temperature and vacuum environment. In addition, it was impossible to confirm whether there were extremely small pores in Ti_2AlC/Mg ceramic phase and whether magnesium alloy infiltrates into the extremely small pores in Ti_2AlC/Mg ceramic phase. The microstructure of three-dimensional interpenetrating network was observed between Ti_2AlC/Mg ceramic phase and AZ91D magnesium alloy phase. The "three-dimensional interlocking" structure between the reinforced phase and the matrix can synergistically enhance the mechanical properties and damping properties of the two phases, thus obtaining composite materials with excellent damping-strength comprehensive properties.

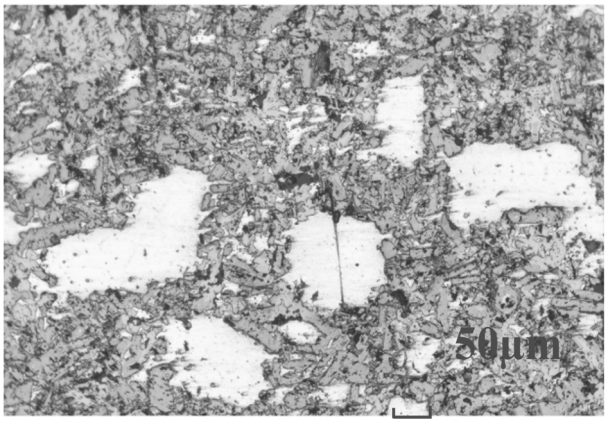

Fig. 3 *Microstructure of three-dimensional network Ti_2AlC/Mg matrix composites under microscopic microscope*

In addition, no new impurity phase was found between the two phases from Fig. 3, but a small amount of hole defects are still found. Therefore, the composite material is not completely dense. And these pores are very unfavorable to the mechanical properties of the composite material.

(3) Interface structure analysis

Scanning electron microscope observation was carried out at the microscopic interface of magnesium alloy matrix/Ti_2AlC/Mg ceramic, and the SEM image obtained was shown in Fig. 4 (A), and the EDS line scanning process was shown in Fig. 4 (B).

From Fig. 4 (A), it can be concluded that magnesium alloy successfully penetrates into the ceramic phase along fine gaps and is widely distributed in the ceramic phase. In Fig. 4 (B), the scanning direction was from left to right. The left part was Ti_2AlC/Mg ceramic phase and the right part was matrix magnesium alloy. Based on the research results of Barsoum et al. [19-20], it can be seen that there was not only no new phase formation at the interface. So it can be determined that the prepared composite material did not have interfacial reaction.

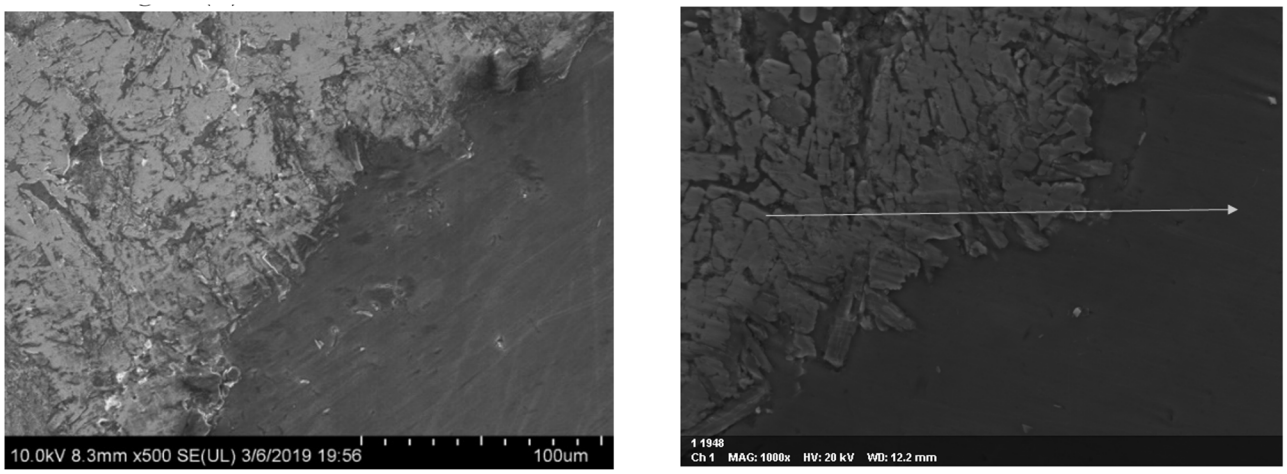

(A) Interfacial morphology of composite materials (B) EDS diagram

Fig. 4 *Interface structure analysis*

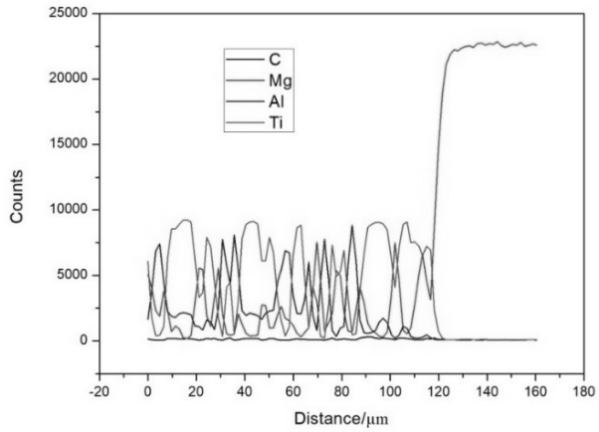

Fig. 5 *Results of line scanning at microscopic interface*

For the Fig. 5, the main elements in the left Ti_2AlC/Mg ceramic region were Mg, Ti and Al, and contained a small amount of element C. However, the matrix region on the right side of the matrix magnesium alloy contained only Mg element. The Mg element curve was at a high level on the right side and drops abruptly at the interface between the matrix and the ceramic. Finally, it reached a low level in the ceramic phase region and continues to fluctuate. This not only shown that there were many fine pores randomly distributed in the ceramic phase, but also the pore size value distribution was uneven. It also shown that magnesium alloy had successfully penetrated into ceramic phase, which was consistent with SEM images.

3.2 Performance analysis

(1) Mechanical properties of Ti_2AlC/Mg matrix composites.

Bending strength has important reference value for measuring the mechanical properties of a material. In order to study the effect of the introduction of composite reinforcing phase on the mechanical properties of matrix magnesium alloy. Bending loads were applied to the matrix magnesium alloy and different positions of the composite material (as shown in the red circle of Fig. 6) by using the three-point bending method, and the bending properties were tested.

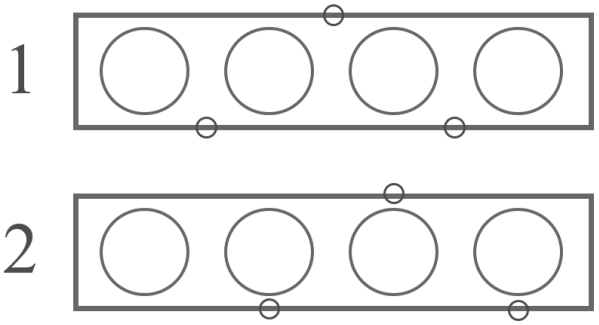

Fig. 6 *Different test points of composite bending experiment*

Typical mechanical property curves of magnesium alloy and composite material samples at test positions 1 and 2 shown in Fig. 6 under flexural load were shown in Figs. 7 (a), (b) and (c). In Fig. 7(A), the bending strength of the composite material had been improved by up to about 10% compared with AZ91D. The bending load curve of the matrix magnesium alloy risen uniformly first. When the bending load reached the bending strength limit of the matrix magnesium alloy, the curve suddenly dropped to the lowest level. When the load was applied to the ceramic part, the bending load curve of the composite sample was quite different from that of magnesium alloy. The curve started to rise rapidly after going through a step-by-step process. When reaching the ultimate bending strength, the curve shown a step-by-step downward trend until the sample was broken. When the test site was facing the magnesium alloy matrix, the bending resistance line of the material sample was different from the second half of the bending resistance line of the No.1 composite sample.

After reaching the bending strength limit, the curve experienced a sudden drop and then began to climb upward. After a considerable period of time, the curve plummeted to its lowest level.

However, from the curves of Figs. 7(B) and (C), even if the bending load borne by the composite material reached its ultimate bending strength, the composite material can still maintain a strength slightly lower than the ultimate bending strength for a considerable period of time thereafter.

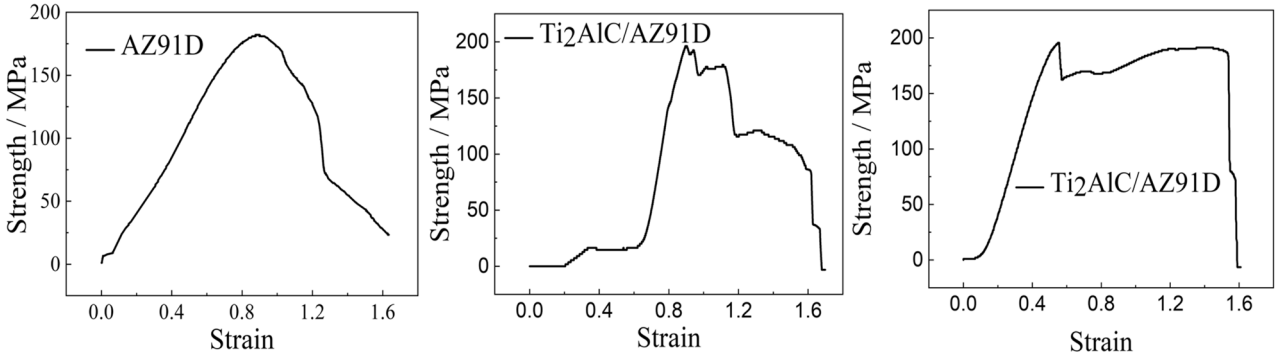

(A) Matrix magnesium alloy sample. (B) No.1 composite specimen. (C) No. 2 composite specimen.

Fig. 7 *Typical mechanical curves of bending load of each sample*

In order to explain the obtained test results, the fracture surfaces of composite materials samples at different test positions were observed by scanning electron microscope, and the scanning positions were shown in Fig. 8.

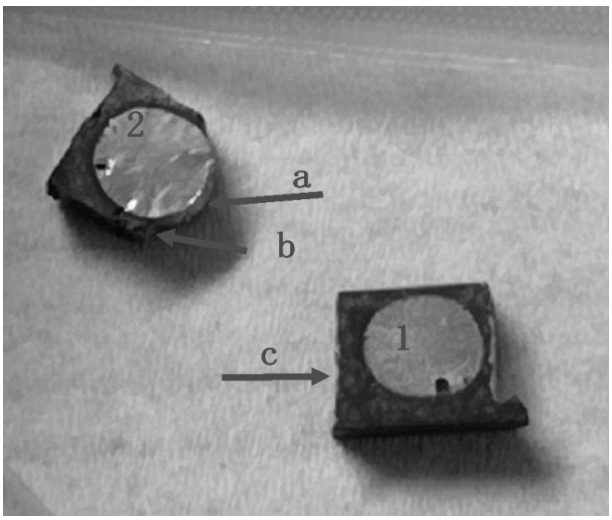

Fig. 8 *Scanning position diagram of electron microscope*

The scanning result of position C in Fig. 8 was shown in Fig. 9 (A). It can be seen that Ti_2AlC/Mg particles were surrounded by "wave" magnesium at the fracture surface of the composite material bent from position C, including tear edges formed on the magnesium alloy matrix after Ti_2AlC/Mg particles were pulled out of the matrix magnesium alloy, and Ti_2AlC/Mg particles that had not been pulled out but had cleavage fracture themselves. This shown that the magnesium liquid successfully penetrates into the microscopic pores along the microscopic gaps in the porous ceramic plate, shrinks slightly during condensation and always binds tightly with Ti_2AlC/Mg particles. Due to the good ductility of magnesium alloy, the magnesium alloy matrix distributed around Ti_2AlC/Mg particles was elongated to form tear edges during the bending process of the composite material. This was the reason why the composite material shown higher strength and better ductility than the ceramic phase. In addition, during the scanning of the c position, a special laminated structure of Ti_2AlC/Mg ceramic particles as shown in Fig. 9 (B) was found. Ti_2AlC/Mg ternary MAX ceramic material was composed of octahedral stacked Ti atomic layer and planar structure Al atomic layer stacked at intervals. Therefore, it was microscopically characterized as a laminated structure. As can be seen from Fig. 9 (B), the laminated directions of each particle were completely different and staggered with each other. This maked the composite material exhibit anisotropy macroscopically. When the laminated structure was subjected to bending stress from the stacking direction, bending will occur and consume bending strain energy, which can effectively resist the bending effect of external force on the composite material.

The scanning result of position b in Fig. 8 is shown in Fig. 10 (A). In the low-power microscopic scanning image, it can be seen that the crack propagation path of ceramic phase was a winding curve instead of a straight line. This was due to the stacking and arrangement of Ti_2AlC/Mg particles in different directions. When the crack propagation direction was the same as the plate-like structure of Ti_2AlC/Mg granular layer, Ti_2AlC/Mg particles will delaminate along the laminar direction, and the crack will continue to move forward along the original direction. When the crack reached other Ti_2AlC/Mg particles with different directions in the lamellar structure, the crack will first penetrate the first few layers of the Ti_2AlC/Mg granular lamellar structure. Then, the crack will lose the ability to continue to advance in the direction perpendicular to the

lamellar structure due to the energy dissipation effect of lamination results. The crack will deflect and continue to propagate along the relatively easy delamination direction of Ti_2AlC/Mg particles. Further, upon further observation of the Ti_2AlC/Mg granular layer plate-like structure at position b in Fig. 8, it was found that the transgranular fracture layered structure had a slight kink (Fig. 10 (B)). When the kink band was subjected to slight external load, the kink band structure will be dislocated under the action of external load, the laminate structure will be bent and deformed, and some layers will be separated. The dislocation structure at this time is called the initial kink band. When the external load on the initial kink band is too large, it will be broken due to excessive deformation. The initial kink band structure will only appear when it is loaded. When it is not loaded, the structure disappears. The deformation mechanism of kink band can consume part of the strain energy brought by external load. Therefore, it has a good contribution to the mechanical properties of composite materials.

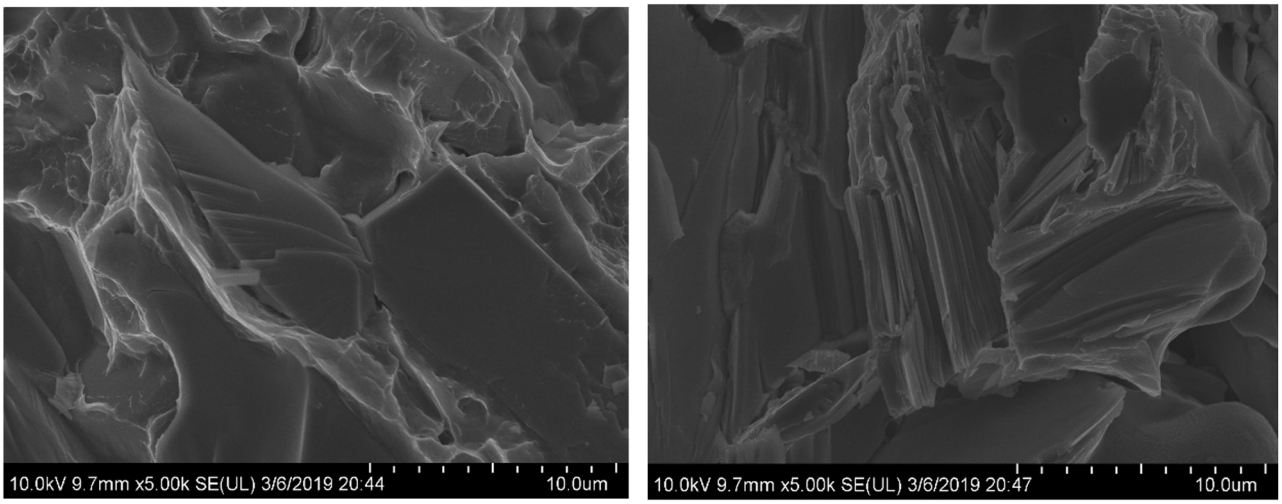

(A) Magnesium alloy matrix and Ti_2AlC/Mg particles. (B) Layered structure of Ti_2AlC/Mg ceramic particles.

Fig. 9 *Scanning electron microscope results at fracture surface at position C*

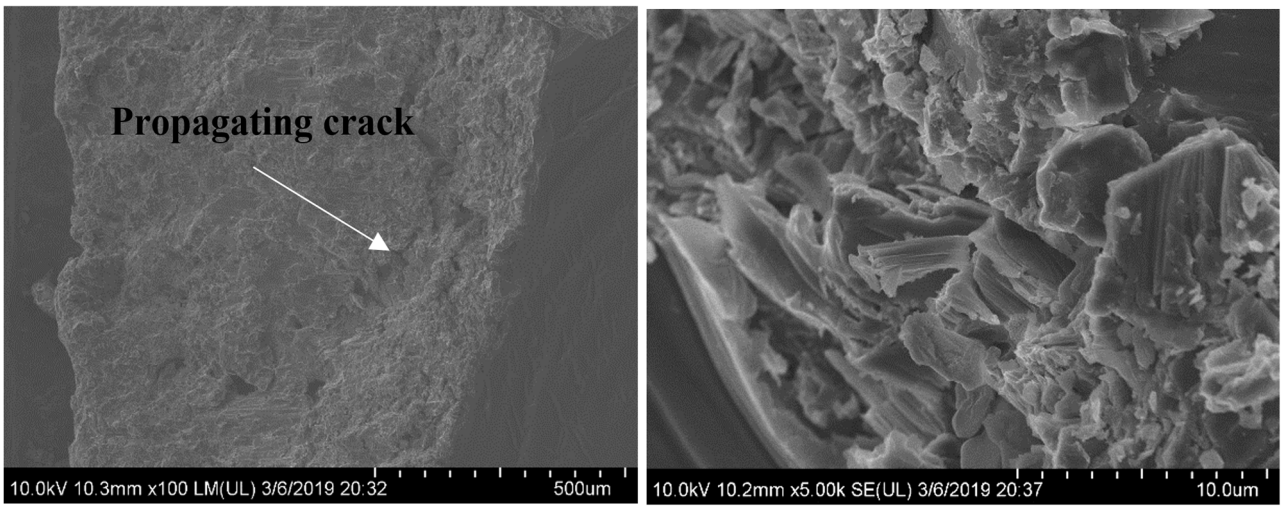

(A) Crack Propagation in Ti_2AlC/Mg Ceramic Phase. (B) Ti_2AlC/Mg particle kink band structure.

Fig. 10 *Scanning electron microscope results at position b*

The microscopic morphology of the fracture at a in Fig. 8 was shown in Fig. 11. From the Fig. 11 (A), it was concluded that the fracture microscopic image at a shown more matrix magnesium alloy than the fracture morphology at composite b. Form the Fig. 11 (A), Ti_2AlC/Mg ceramic was surrounded by matrix magnesium alloy, the structure with "wave" tear ribs was matrix magnesium alloy, and the regular structure with smooth plane was Ti_2AlC/Mg ceramic. There were some incompact areas between matrix magnesium alloy and ceramic reinforcement phase, which catalyzes crack propagation.

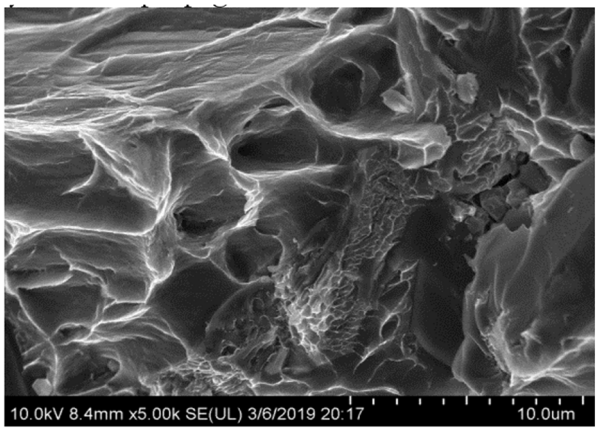

(A) Ductile fracture magnesium alloy and Ti_2AlC/Mg particles.

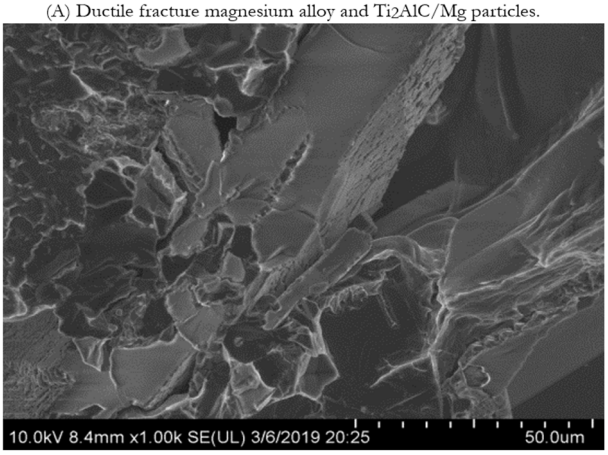

(B) The comprehensive fracture mechanism of No. 2 composite specimens.

Fig. 11 *SEM results of fracture at position a*

In order to further study the fracture mechanism of composite material No.2 sample, the microscopic morphology Fig. 11 (B), which can show the comprehensive fracture mechanism of composite material No.2 sample, was obtained after further observation of the fracture surface. It can be seen that the fracture mechanism of No.2 composite material consists of three fracture forms: ductile tearing of matrix magnesium alloy, fracture of Ti_2AlC/Mg ceramic and partial fracture of magnesium alloy/ceramic along the interface. The main fracture forms of the composite material were ductile fracture of matrix magnesium alloy and transgranular fracture of Ti_2AlC/Mg ceramic plate particles perpendicular to its laminated structure. The second was partial fracture along the interface, and obvious cracks were generated between the matrix/ceramic phase interface. This shown that Ti_2AlC/Mg ceramics, matrix magnesium alloy and the two-phase interface inside the composite can consume the strain energy of the material through cracking.

(2) Study on damping properties of Ti_2AlC/Mg matrix composites with double-scale three-dimensional network.

The damping properties of double-scale three-dimensional network composites at 1Hz and 10Hz were measured at different temperature points. The test strain amplitude was 0.01 mm, the test temperature range was 20℃~300℃, and the heating rate was 5 K/min. The obtained damping-temperature spectrum curves at different frequencies were shown in Figs. 12 and 13.

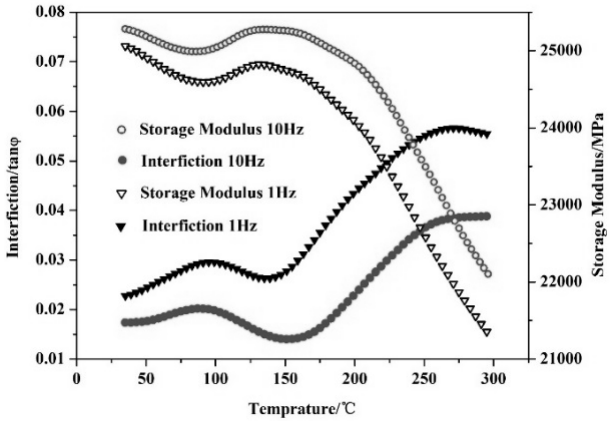

Fig. 12 *Damping-temperature spectrum curve of AZ91D magnesium alloy*

For the Fig. 12, the storage modulus of AZ91D magnesium alloy was about 21 GPa ~ 26 GPa, which was at a relatively low level. At higher excitation frequency, the storage modulus of magnesium alloy was relatively higher. When the temperature risen to about 150℃, the storage modulus of the material decreased sharply. This was consistent with the poor high temperature performance of AZ91D magnesium alloy, indicating that the material was generally used in the temperature range below 150℃. Judging from the internal friction value, the test frequency had a great influence on the internal friction value of magnesium alloy. At the test frequency of 1Hz, its internal friction value was relatively high, in the range of 0.02~0.06, showing higher damping power compared with common metal materials. When the test frequency was 10Hz, the internal friction value decreases significantly and was in the range of 0.014~0.04. The damping variation law of magnesium alloy was relatively consistent at different frequencies, and obvious damping peaks appear at about 100℃, showing obvious grain boundary damping peaks. This was due to the sliding of grain boundaries under the action of high temperature. There was a wide damping peak in the temperature range of 80℃~100℃, showing good damping ability. When the temperature continued to rise to 150℃, the storage modulus decreased sharply due to the softening of the alloy, while the loss factor increased significantly. The material cannot give full play to the characteristics of high damping ability because it cannot meet the requirements of strength performance. On the whole, AZ91D magnesium alloy had good potential application in the temperature range

below 100℃, its internal friction value was in the medium range of 0.015~0.03, and its storage modulus was about 25 GPa.

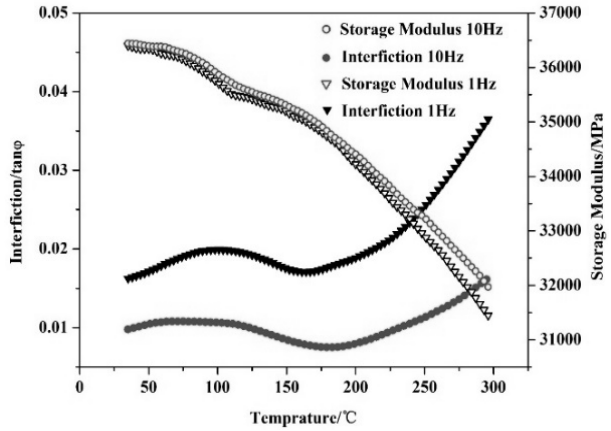

Fig. 13 *Damping-temperature curve of double-scale three-dimensional network Ti_2AlC/Mg matrix composites*

The damping-temperature spectrum curve of the composite material was given by Fig. 13. In the temperature range tested by the experiment, the storage modulus of the composite material was between 31 GPa and 36 GPa, which was not only at a high level but also did not show steep slope decline. This shown that the addition of ceramic phase not only had good strengthening effect, but also due to the thermal mismatch strain at the interface. The residual internal stress caused by this also contributes to the storage modulus. The storage modulus of composite materials was very close at different test frequencies, which shown that the vibration frequency has little influence on the storage modulus. Judging from the internal friction value, the damping performance of the composite material at 1Hz was obviously better than that at 10 Hz. Under the test condition of 1Hz, the internal friction value of the material was only in the lower level of 0.01~0.156, while under the condition of 10 Hz, the internal friction value of the material was in the range of 0.16 ~ 0.38. Although the damping performance of the composite material fluctuates and produces an internal friction peak at 100℃, it increased with the increase of temperature as a whole.

3.3 Model reconstruction and performance prediction of composite materials based on double-scale three-dimensional network structure

In this experiment, spherical-like stearic acid particles after ball milling were used to form pores, so the pores of the microscopic porous Ti_2AlC/Mg ceramics prepared shown spherical-like structure. The diameters of the holes were dispersed and randomly distributed. In the later stage of this experiment, magnesium liquid was immersed into these microscopic pores, and a three-dimensional network structure in which the positions of microscopic pores were occupied by magnesium alloy AZ91D was obtained. Therefore, this study is carried out by model establishment and finite element method simulation.

In this paper, the microstructure of Ti_2AlC/Mg matrix composites (100 m × 100 m × 100 m) was modeled by ANSYS APDL module. With the help of SEM images of Ti_2AlC/Mg microscopic porous three-dimensional network ceramics, it can be seen that the diameter of spherical pores was mainly concentrated between 20 m and 40 m. Therefore, the magnesium matrix in the composite material was equivalent to spherical, and the periodic volume characterization model of the composite material with AZ91D content of 40vol% was established by using APDL module of ANSYS software. The model was shown in Fig. 14 (A). The coupling settings were shown in Fig. 14 (B). After calculation, an equivalent stress nephogram as shown in Fig. 14 (C) was obtained.

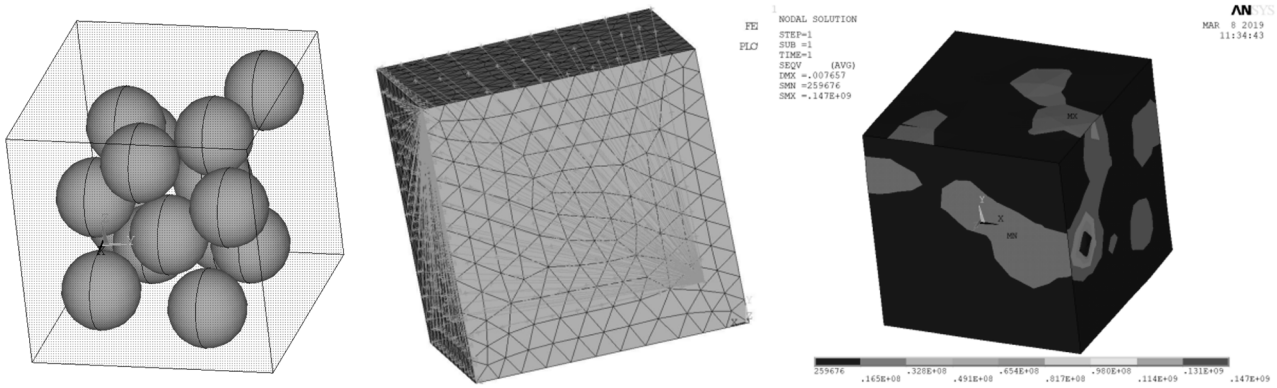

（A）Modeling （B）Coupling Settings （C）Equivalent stress

Fig. 14 *Microscopic equivalent model analysis of composite materials*

In Fig. 14 (C), the stress was concentrated in the spherical magnesium inside the model and its interface with ceramics, which was consistent with the actual situation. The volume, equivalent stress and equivalent strain of each element of the model were extracted by using the finite element method and directly according to the RVE (representative volume element) simulation results of the composite material, and then brought into the Eqs. (3)-(5) to obtain the equivalent modulus of the composite material.

$$\sigma = \frac{1}{V_C}\sum_{i=1}^{n}\sigma_i v_i \quad (3)$$

$$\varepsilon = \frac{1}{V_C}\sum_{i=1}^{n}\varepsilon_i v_i \quad (4)$$

$$E = \frac{\sigma}{\varepsilon} \quad (5)$$

The final equivalent elastic modulus of the composite material was 31.26 GPa. The simulation results shown that the maximum storage modulus of the composite material was 36.40 GPa and the minimum was 31.37 GPa. Compared with the stored modulus measured by experiments, the maximum error of the calculated equivalent modulus was about 16%, and the minimum error was about 0.4%. The calculated results were in good agreement with the experimental results, which shown that the calculation method was reasonable.

4 Conclusion

(1) Through the research on the preparation process parameters and microstructure of the composite material, capillary force on magnesium liquid infiltration of porous ceramic plates played a positive role in its infiltration under negative pressure. Macroscopically, the prepared composite material was homogeneous and free of defects such as pores and cracks. Microscopically, the interface between Ti_2AlC/Mg ceramic phase and matrix magnesium alloy was good, and magnesium alloy successfully penetrated into the gaps between Ti_2AlC/Mg ceramic particles. According to the results of EDS composite interface line scanning, there was no reaction between matrix magnesium alloy and Ti_2AlC/Mg ceramic during magnesium liquid infiltration.

(2) The mechanical properties and damping properties of Ti_2AlC/Mg matrix composites and magnesium alloy matrix prepared by double-scale three-dimensional network were tested. According to the basic properties of Ti_2AlC/Mg ceramics and AZ91D, the equivalent modulus of the three-dimensional network Ti_2AlC/Mg matrix composites on the microscopic scale was predicted by finite element method. The following conclusions were drawn: the ultimate bending strength of the composites was increased by about 10% compared with the matrix magnesium alloy, and the ability to maintain the strength was greatly improved compared with the matrix magnesium alloy.

(3) The ANSYS APDL command was used to reconstruct the microscopic model of the composite material, set the loading, solve it, and extract the element stress, strain and other information of the deformed microscopic model. Finally, using the extracted information, the equivalent modulus of the composite microscopic model was calculated to be 31.26 GPa, which was consistent with the experimental results and provided a theoretical basis for the optimization of the pore structure of the composite material in the next step.

Acknowledgement

This work was supported by the Sichuan Science and Technology Program (2021YFG0019).

References

[1] KOŠTIALIKOVÁ D, JANEKOVÁ M, DUBEC A, KOVÁČIKOVÁ P. (2022). Stent Wear Analysis for Percutaneous Coronary Interventions[J]. *Manufacturing Technology,* 22(2):180-184

[2] ZYSKA A, BOROŃ K. (2021). Comparison of the Porosity of Aluminum Alloys Castings Produced by Squeeze Casting[J]. *Manufacturing Technology,* 21(5):725-734

[3] GRANATO A, LUCKE K. (1956). Theroy of mechanical damping due to dislocation [J]. *J. Appl. Phys*, 27 (6): 583-593

[4] UHRÍČIK M, DRESSLEROVÁ Z, PALČEK P, CHALUPOVÁ M, HANUSOVÁ P. (2019). Analysis of Amplitude Dependence of Internal Damping of AZ31 and AZ61 Alloys in Initial State and after Deformation[J]. *Manufacturing Technology,* 19(6):1047-1053

[5] SRIKANTH N, ZHONG X L, GUPTA M. (2005). Enhancing damping of pure magnesium using nano-size alumina particulates[J].*Materials Letters*, 59(29-30):3851-3855

[6] CAO W, ZHANG C, FAN T. (2008). In situ synthesis and damping capacities of TiC reinforced magnesium matrix composites [J]. *Composits Science and Engineering:A*, 496(1-2):242-246

[7] ZHANG X, WANG H, LIAO L. (2007). In situ synthesis method and damping characterization of magnesium matrix composites[J].*Materials Science and Technology*, 67(3):720-727

[8] WU Y W, WU K, DENG K K. (2010). Damping capacities and tensile properties of magnesium matrix composites reinforced by graphite particles[J].*Materials Science and Engineering: A,* 527(26):6816-6821

[9] WU Y W, WU K, DENG K K. (2010). Damping capacities and microstructures of magnesium matrix composites reinforced by graphite particles[J].*Materials & Design*, 31(10):4862-4865

[10] GU J, ZHANG X, QIU Y. (2005). Damping behaviors of magnesium matrix composites reinforced with Cu-coated and uncoated SiC particulates[J].*Composites Science and Technology*, 65(11): 1736-1742

[11] KONTSOS A, LOUTAS T, KOSTOPOULOS V. (2011). Nanocrystalline Mg–MAX composites: Mechanical behavior characterization via acoustic emission monitoring[J].*Acta Materialia*, 59(14): 5716-5727

[12] SHAHRAM A, BARSOUM M W. (2010). On the effect of texture on the mechanical and damping properties of nanocrystalline Mg-matrix composites reinforced with MAX phases[J].*Materials Science and Engineering:A*, 527(16-17): 3707-3718

[13] ZHANG C, FAN T, CAO W. (2009). (AlN+Mg2Si)/Mg composites in situ synthesis and scale effect of particulate on damping capacity[J].*Materials Science and Engineering: A*, 508(1):190-194

[14] TROJANOVÁ Z, LUKÁC P, RIEHEMANN W. (2009). Damping behaviour of a Mg–Al–Ca alloy reinforced by short Saffil fibres[J].*Materials Science and Engineering A*, 521-522 (36): 314-317

[15] XIONG B, YU H, XU Z. (2011). Fabrication of SiC particulate reinforced AZ91D composite by vacuum-assisted pressure infiltration technology[J]. *Journal of Alloys & Compounds*, 509(29):L279-L283

[16] NOVÁ I, FRAŇA K, SOBOTKA J, SOLFRONK P, KOREČEK D, NOVÁKOVÁ I. (2019). Production of Porous Aluminium Using Sodium Chloride[J]. *Manufacturing Technology,* 19(5):817-822

[17] YU HUASHUN. (2001). Metal Matrix Composites and Their Preparation Technology [M]. *Beijing: Chemical Industry Press*

[18] LI RONGJIU. (2003). Ceramic-metal composite materials [M]. *Beijing: Metallurgical Industry Press*

[19] ANASORI B, CASPIL E N, BARSOUM M W. (2014). Fabrication and mechanical properties of pressureless melt infiltrated magnesium alloy composites reinforced with TiC and Ti2AlC/Mg particles[J].*Materials Science and Engineering:A*,618(11):511-522

[20] ANASORI B, BARSOUM M W. (2016). Energy damping in magnesium alloy composites reinforced with TiC or Ti2AlC/Mg particles [J].*Materials Science & Engineering A*, 653(1): 53-62